Available online at www.sciencedirect.com
SCIENCE DIRECT®
Scripta Materialia 55 (2006) 295–297
Scripta MATERIALIA
www.actamat-journals.com

Polymer-derived SiAlCN ceramics resist oxidation at 1400 °C

Yiguang Wang,[a] Yi Fan,[b] Ligong Zhang,[b] Wenge Zhang[c] and Linan An[a,*]

[a] *Advanced Materials Processing and Analysis Center, University of Central Florida, 4000 Central Florida Blvd, Orlando, FL 32816, USA*
[b] *Laboratory of Excited State Process, Changchun Institute of Optics, Fine Mechanics and Physics, Chinese Academy of Sciences, Changchun 130032, China*
[c] *Sporian Microsystem Technology Inc., Boulder, CO 80026, USA*

Received 6 February 2006; revised 28 April 2006; accepted 5 May 2006
Available online 26 May 2006

The oxidation kinetics of polymer-derived SiAlCN ceramics are determined at 1400 °C by measuring oxide-scale thickness as a function of oxidation time. The results reveal that the SiAlCN ceramics possess much better oxidation resistance than polymer-derived SiCN without Al, pure SiC and Si_3N_4. X-ray diffraction studies reveal that the oxide scales consist of cristobalite, plus a small amount of mullite for the sample with high aluminum-content. The reason that the SiAlCNs exhibited better oxidation resistance is discussed.
© 2006 Acta Materialia Inc. Published by Elsevier Ltd. All rights reserved.

Keywords: SiAlCN; Oxidation; Precursor

Silicon-based non-oxide ceramics such as SiC and Si_3N_4 are currently considered as structural materials for high-temperature applications due to their excellent thermomechanical properties [1]. Traditionally, these materials are prepared by sintering corresponding powders with oxide sintering aids such as Y_2O_3 and/or Al_2O_3, which promote densification by forming liquid phases at sintering temperatures. However, the same liquid phases result in severe high-temperature property degradation and limit the applications of the materials. Alternatively, these materials can be synthesized by thermal decomposition of polymeric precursors, referred to as polymer-derived ceramics (PDCs). This direct chemical-to-ceramic route possesses many advantages over traditional powder-based ceramic processing. For example, the technique leads to a simple and cost-efficient approach to manufacturing of ceramic components and devices in useful shapes, such as fibers, coatings, composites, micro-electro-mechanical system (MEMS) and nanostructures [2–5]. While synthesized at relatively low-temperatures (pyrolysis is usually performed at 800–1000 °C), PDCs show excellent high-temperature properties, such as resistance to creep [6–9] and to large-scale crystallization [10], thus showing promise for applications at elevated temperatures.

The structural materials assigned to high-temperature applications in oxygen-containing environments must embody excellent resistance to oxidation. Therefore, the oxidation behavior of PDCs has been the subject of several previous studies [11–16]. It was found that the polymer-derived ceramics of Si–C–N and Si–B–C–N systems exhibited similar oxidation resistance to conventional silicon carbide and silicon nitride [17]. Recently, An and co-workers reported that polymer-derived SiAlCN ceramics exhibited much better oxidation and hot-corrosion resistance than other silicon-based ceramics at temperatures up to 1200 °C [18–20].

In this paper, the oxidation behavior of the polymer-derived SiAlCN ceramics is studied at 1400 °C with the objective of seeing if the excellent oxidation resistance of the SiAlCNs can be retained at higher temperatures where the oxide scale transforms to crystalline phases instead of amorphous phases.

Fully dense polymer-derived SiAlCN and SiCN discs were prepared by using a pressure-assisted pyrolysis technique described previously [4]. For the SiCN, commercially available polyurea(methylvinyl)silazanes (PUMVS) were used as the precursor. For the SiAlCNs, the precursors were polyaluminasilazanes, which were synthesized by reaction of PUMVS and aluminum

* Corresponding author. Tel.: +1 4078231009; fax: +1 4078230208; e-mail: lan@mail.ucf.edu

1359-6462/$ - see front matter © 2006 Acta Materialia Inc. Published by Elsevier Ltd. All rights reserved.
doi:10.1016/j.scriptamat.2006.05.004

Table 1. Precursors and compositions of obtained ceramics

Materials	Starting materials (PUMVS:AIP)	Ceramic compositions
SiCN	100:0	$SiC_{0.99}N_{0.85}$
SiAlCN-10	90:10	$SiAl_{0.04}C_{0.83}N_{0.93}$
SiAlCN-20	80:20	$SiAl_{0.08}C_{0.80}N_{0.95}$
SiAlCN-30	70:30	$SiAl_{0.12}C_{0.78}N_{0.91}$

isopropoxide (AIP) using procedures described in Ref. [21]. Three types of SiAlCNs containing different amounts of aluminum were synthesized by varying the ratio of PUMVS to AIP. The ceramics obtained were amorphous in nature, and their chemical compositions were measured and are listed in Table 1. The samples also contain less than 3 wt.% oxygen.

For oxidation studies, one side of the disk was polished to 0.5 μm finish using diamond-lapping films. The sample was then put in a high-purity alumina combustion boat with the polished side facing up. The oxidation was carried out in a high-temperature tube furnace in flowing dry air at 1400 °C for various oxidation times up to 200 h. After oxidation, the pre-polished surface of the specimen was glued to a thin glass slide using Epoxybond 110™ to protect it from possible damage during further machining. A cross-section was cut from the specimen and polished to 0.5 μm finish using diamond-lapping films and etched using buffered oxide etchants to delineate the oxide layer from the substrate.

The oxide scales were observed using scanning electron microscopy (SEM), and their thickness was measured from the SEM images. The crystal structures of the oxide scales were characterized using X-ray diffraction (XRD).

The oxide scales were first examined by observing the cross-section of oxidized samples under SEM. Figure 1 shows a typical SEM image of the cross-section of an oxidized specimen. The observations reveal that all oxide scales are dense and free of bubbles and cracks regardless of oxidation times and substrate materials. The thickness of the oxide scale is uniform through the sample.

The thickness of the oxide scale was measured from SEM images. Figure 2 plots the square of the thickness of the oxide scale (h^2) as a function of oxidation time t. It can be seen that SiCN obeys typical parabolic kinetics (linear relationship between h^2 and t). While the linear

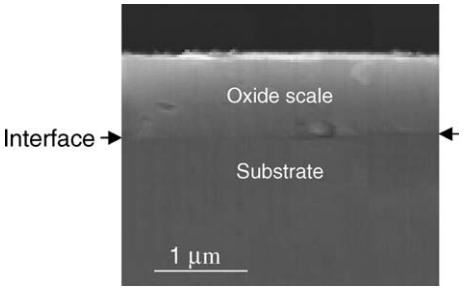

Figure 1. SEM image obtained for SiAlCN-10 ceramic oxidized for 20 h, showing the typical morphology of the cross-section of an oxidized sample.

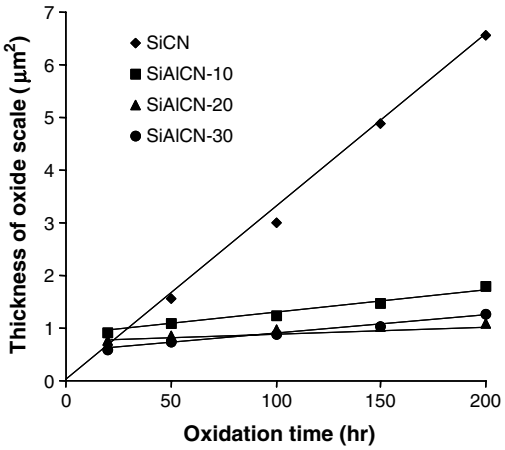

Figure 2. The square of the thickness of the oxide scale as a function of oxidation time for SiCN, SiAlCN-10, SiAlCN-20 and SiAlCN-30.

dependences of h^2 on t are also observed for the three SiAlCN specimens, the extrapolations of the lines have positive intercepts with the y-axis. This suggests that the oxidation rates of the SiAlCNs are much higher in the short-term than in the long-term. The similar asymmetric oxidation behavior has also been observed for the SiAlCNs at lower temperatures of 1000–1200 °C [19]. It was found that in the lower temperature range the oxide scales were Al-doped amorphous silica, and the asymmetric oxidation was due to rearrangement of aluminum positions with oxidation times.

The parabolic oxidation rate constants, k_p, can be measured from the slope of the lines presented in Figure 2 according to the expression [22]:

$$h^2 = k_p t \tag{1}$$

where h is the thickness of the oxide scale and t the annealing time. The measured oxidation rates for SiCN and the SiAlCNs are summarized in Table 2, together with the lowest oxidation rates of other silicon-based ceramics reported previously, which were measured from chemical vapor deposited (CVD) SiC and Si_3N_4 [23]. It can be seen that the oxidation rate of SiCN is close to those of CVD SiC and Si_3N_4. However, the SiAlCNs exhibit lower oxidation rates. It can also be noted from the table that the oxidation rates of the SiAlCNs depended on aluminum content. The SiAlCN-20, in which the ratio of Si to Al is ~1:0.08, shows the lowest oxidation rate, which is more than an order of

Table 2. Comparison of oxidation rates and lattice parameters of cristobalite between different silicon-based ceramics

	$k_p \times 10^{18}$ (m²/s)	Lattice constants of cristobalite (nm)	
		a	c
SiCN	9.7	0.4936	0.6780
SiAlCN-10	1.2	0.4939	0.6960
SiAlCN-20	0.47	0.4979	0.7104
SiAlCN-30	1	0.4946	0.7007
CVD SiC [23]	16.4	–	–
CVD Si_3N_4 [23]	6.2	–	–

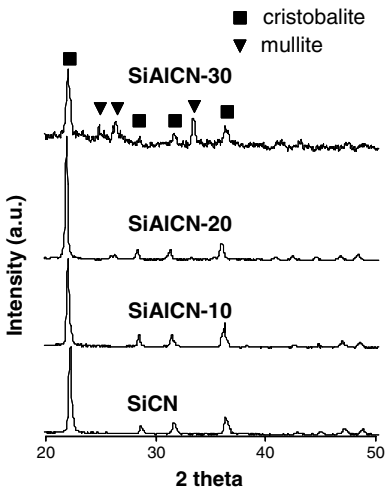

Figure 3. XRD patterns of SiCN, SiAlCN-10, SiAlCN-20 and SiAlCN-30 oxidized at 1400 °C for 200 h.

magnitude lower than those for all other silicon-based ceramics.

For further understanding of the oxidation behavior of the SiCN/SiAlCNs, the oxide scales were characterized using XRD. The results (Figure 3) reveal that the oxide scales are crystalline. For SiCN and SiAlCN-10 the oxide scales were cristobalite only; for SiAlCN-30 the oxide scale consisted of mullite in addition to a major cristobalite phase; and the oxide scale of the SiAlCN-20 also contained a very small amount of mullite besides cristobalite. The XRD patterns were used to calculate lattice parameters of the cristobalite formed on different substrates and the results are listed in Table 2. It can be seen that the presence of aluminum caused an increase in the lattice parameters, suggesting that aluminum dissolved into the cristobalite. The cristobalite formed on SiAlCN-20 showed larger lattice parameters than that formed on SiAlCN-10 and is due to the former having a higher aluminum concentration. The cristobalite that formed on SiAlCN-30 had smaller lattice parameters than that formed on SiAlCN-20 and is likely due to the formation of mullite, which consumed aluminum and results in a lower aluminum concentration in the cristobalite.

A recent study [24] clearly demonstrated that the oxygen transportation mechanism in cristobalite is the same as in amorphous silica, which is oxygen molecule diffusion through six-membered SiO_4 rings [25]. Consequently, we propose that the better oxidation resistance exhibited by the SiAlCNs is due to the aluminum atoms dissolving in cristobalite and blocking the rings, leading to a decrease in the diffusion rate of oxygen. The more aluminum atoms dissolved in the cristobalite, the lower the oxidation rate becomes. We further propose that the formation of the unique structure where aluminum atoms block the six-membered SiO_4 rings of cristobalite occurred gradually, which led to the asymmetric oxidation kinetics in the short-term (Figure 2). This is similar to what occurred at lower temperatures [19]. However, it took much longer times (50–100 h) to rearrange aluminum into equilibrium positions at lower temperatures [19] than at 1400 °C (<20 h).

The oxidation behavior of polymer-derived SiCN and SiAlCN ceramics has been studied at 1400 °C. The results show that the SiAlCN ceramics exhibit a much better oxidation resistance. The lowest oxidation rate observed for SiAlCN-20 is more than an order of magnitude lower than the lowest values reported in the literature for pure SiC and Si_3N_4. A structural model where aluminum atoms block the oxygen diffusion in cristobalite is proposed to account for the observed phenomena.

This work is financially supported by DOE-NETL (program manager, Dr. S. Maley).

[1] K.H. Jack, J. Mater. Sci. 11 (6) (1976) 1135.
[2] S. Yajima, Y. Hasegawa, K. Okamura, T. Matsuzawa, Nature 273 (1978) 525.
[3] L. An, W. Xu, S. Rajagopalan, C. Wang, H. Wang, J. Kapat, L. Chow, Y. Fan, L. Zhang, D. Jiang, B. Guo, J. Liang, R. Vaidyanathan, Adv. Mater. 16 (22) (2004) 2036.
[4] L. Liew, W. Zhang, L. An, S. Shah, R. Lou, Y. Liu, T. Cross, K. Anseth, V. Bright, R. Raj, Am. Ceram. Soc. Bull. 80 (5) (2001) 25.
[5] W. Yang, H. Miao, Z. Xie, L. Zhang, L. An, Chem. Phys. Lett. 383 (5–6) (2004) 441.
[6] L. An, R. Riedel, C. Konetschny, H.J. Kleebe, R. Raj, J. Am. Ceram. Soc. 81 (1998) 1349.
[7] R. Riedel, L.M. Ruwisch, L. An, R. Raj, J. Am. Ceram. Soc. 81 (1998) 3341.
[8] M. Christ, G. Thurn, M. Weinmann, J. Bill, F. Aldinger, J. Am. Ceram. Soc. 83 (2000) 3025.
[9] A. Zimmermann, A. Bauer, M. Christ, Y. Cai, F. Aldinger, Acta Mater. 50 (2002) 187.
[10] R. Riedel, A. Kienzle, W. Dressler, L.M. Ruwisch, J. Bill, F. Aldinger, Nature 382 (1996) 796.
[11] A. Saha, S. Shah, R. Raj, J. Am. Ceram. Soc. 87 (2004) 1556.
[12] L. Bharadwaj, Y. Fan, L. Zhang, D. Jiang, L. An, J. Am. Ceram. Soc. 87 (2004) 483.
[13] E. Butchereit, K.G. Nickel, A. Muller, J. Am. Ceram. Soc. 84 (2001) 2184.
[14] R. Raj, L. An, S. Shah, R. Riedel, C. Fasel, H.J. Kleebe, J. Am. Ceram. Soc. 84 (2001) 1803.
[15] H.P. Baldus, M. Jansen, Angew. Chem. Int. Ed. Engl. 36 (1997) 328.
[16] D. Mocaer, G. Chollon, R. Pailler, L. Filipuzzi, R. Naslain, J. Mater. Sci. 28 (1993) 3059.
[17] N.S. Jacobson, E.J. Opila, K.N. Lee, Curr. Opin. Solid State Mater. Sci. 5 (2001) 301.
[18] L. An, Y. Wang, L. Bharadwaj, L. Zhang, Y. Fan, D. Jiang, Y.H. Sohn, V.H. Desai, J. Kapat, L. Chow, Adv. Eng. Mater. 6 (2004) 337.
[19] Y. Wang, Y. Fan, L. Zhang, S. Burton, Z. Gan, L. An, J. Am. Ceram. Soc. 88 (2005) 3075.
[20] Y. Wang, W. Fei, L. An, J. Am. Ceram. Soc. 89 (2006) 1079.
[21] A. Dhamne, W. Xu, B. Fookes, Y. Fan, L. Zhang, S. Burton, J. Hu, J. Ford, L. An, J. Am. Ceram. Soc. 88 (2005) 2415.
[22] B.E. Deal, A.S. Grove, J. Appl. Phys. 36 (1965) 3770.
[23] L.U.J.T. Ogbuji, E.J. Opila, J. Electrochem. Soc. 142 (1995) 925.
[24] E.C. Ramberg, W.L. Worrell, J. Am. Ceram. Soc. 84 (2001) 2607.
[25] T. Bakos, S.N. Rashkeev, S.T. Pantelides, Phys. Rev. Lett. 88 (2002) 055508.